scientific reports

Check for updates

OPEN

Decoupling chemical and mechanical signaling in colorectal cancer cell migration

Maxwell G. Tetrick[1], Md. Abul Bashar Emon[2], Umnia Doha[2], Marsophia Marcellus[1], Joseph Symanski[2], Valli Ramanathan[3], M. Taher A. Saif[2] & Catherine J. Murphy[1]✉

Colorectal cancer metastasis is governed by a variety of chemical and mechanical signaling that are largely influenced by cancer-associated fibroblasts (CAFs) in the tumor microenvironment. Here, we deconvolute the chemical from mechanical signaling in the case of the colon cancer cell line HCT-116 and CAFs. We examined three chemoattractants (CXCL12, TGF-β, and activin A) which allegedly are secreted by CAFs and induce HCT-116 cell migration. None of the chemoattractants tested resulted in enhanced migration of HCT-116 in a 2D transwell assay, at low cell density. Similarly, CAF-conditioned media also did not lead to enhanced HCT-116 migration, while CAFs co-cultured in the transwell assay did lead to increased HCT-116 migration. This result suggests that either high cell densities are required for chemotaxis, and/or a reciprocal two-way signaling network between CAFs and HCT-116 is necessary to induce chemotaxis. Surprisingly, we find that HCT-116 cells exhibit enhanced migration along the axis of mechanical stress in a 3D collagen matrix, at very high cell densities. This migration is independent of whether the strain is induced mechanically or by CAFs. By comparing purely mechanical and purely chemical migration to a 3D co-culture of CAFs and HCT-116 containing both chemical and mechanical cues, it is concluded that HCT-116 migration is dominated by mechanical signaling, while chemical cues are less influential.

Colorectal cancer is currently the second leading cause of cancer deaths and the third most diagnosed cancer worldwide[1–5]. Recently, there have been growing diagnoses of colon cancer in younger people which has been cause for concern, and colon cancer prevalence overall is expected to double in the coming decade[2,3]. While earlystage diagnosis is the optimal preventative measure, colon cancer detected at later stages, associated with cancer metastasis, has poorer outcomes[1–3,5].

It is now well documented that cancer metastasis and cancer cell migration are greatly influenced by the local tumor microenvironment; changes in the physical and chemical properties of the extracellular matrix (ECM) have been shown to affect cancer cell invasiveness and overall tumor metastasis[6–14]. This ECM remodeling has been largely attributed to cells, such as cancer associated fibroblasts (CAFs), located in the ECM around the tumor site restructuring the local microenvironment[15–20]. CAFs have similarly been implicated in the progression and invasiveness of colorectal cancer cell lines[21,22]. CAFs have been shown to stiffen the ECM as well as secrete various growth factors and chemoattractants that can promote cancer cell migration. However, whether and how the tumor microenvironment governs the crosstalk between cancer cells and CAFs is still unclear.

HCT-116 and other colorectal cancer cell lines have been reported to exhibit increased migration upon exposure to various chemoattractants secreted by CAFs in the ECM[22–26]. Three of these chemoattractants are the chemokine CXCL12, activin A and TGF-β from the TGF-β protein superfamily[22,25,27–30]. CXCL12 has been shown to have elevated levels of expression at tumor perimeter sites in patients with colorectal cancer and is associated with poor survivability[25,29]. Activin A released by CAFs has been shown to enhance the migratory behavior in the colorectal cancer cell line FET[22]. Similarly, TGF- β has been shown to directly increase the migration of HCT-116 cells in vitro[28]. Additionally, it has been reported that some potential chemoattractants require cofactors to promote metastatic behavior in cancer cells[31–33]. Thus, we sought to characterize the response of HCT-116 cells to CXCL12, activin A, and TGF-β to investigate how their combinations may lead to chemically-induced colorectal cancer metastasis.

While CAF secretions have been implicated in cancer cell migration, CAFs themselves exert mechanical force on the tumor microenvironment that promotes migration in various cancer types including colorectal

[1]Department of Chemistry, University of Illinois Urbana-Champaign, Urbana, IL 61801, USA. [2]Department of Mechanical Science and Engineering, University of Illinois Urbana-Champaign, Urbana, IL 61801, USA. [3]Department of Chemical and Biomolecular Engineering, University of Illinois Urbana-Champaign, Urbana, IL 61801, USA. ✉email: murphycj@illinois.edu

cancer. CAFs can stiffen the ECM with collagen crosslinkers as well as mechanically align and stretch collagen fibers in the tumor microenvironment which leads to enhanced cancer cell migration and promotes an epithelial to mesenchymal transition[34–37]. Tumor progression is generally associated with stiffening of the tumor microenvironment and pro-metastatic behavior[38]. This behavior has also been characterized in vitro by increasing the stiffness in an artificial 3D tumor matrix with various additives[39–43]. However, it is not yet known how HCT-116 cells respond to CAF-induced stiffening of the ECM.

In this work, we aim to deconvolute the chemical and mechanical control of HCT-116 migration. By comparing HCT-116 migration in a 3D CAF co-culture to the chemotactic behavior of HCT-116 to various chemoattractants and CAF secretions, we profile chemically driven HCT-116 migration. Similarly, by comparing co-culture migration to HCT-116 migration in an artificially strained ECM, we demonstrate the mechanically dependent nature of colorectal cancer metastasis. A better understanding of the nature of cancer metastasis can inform research into future therapeutics to improve survivability.

Materials and methods

Materials

Human colorectal cancer cells (HCT-116) and cancer associated fibroblasts (CAF05) were obtained from ATCC and Neuromics, respectively. McCoy's 5a complete cell culture media used for HCT-116 cell culture was prepared in house and supplemented with 10% fetal bovine serum (FBS, Sigma-Aldrich) and 1% penicillin and streptomycin. CAFs were cultured in either Vitroplus III low serum (Neuromics) or MSC-GRO low serum (Vitro Biopharma) complete cell media. Chemoattractants CXCL12, TGF-β, and activin A were obtained from Sigma Aldrich. Type I collagen was purchased from Advanced Biomatrix (bovine, 3 mg/mL). Transwell chemotaxis assays were obtained from Millipore Sigma. 3D chemotaxis μ-slides were purchased from Ibidi, and image analysis was conducted in ImageJ.

Cell culture

HCT-116 human colorectal cancer cells were cultured in a 75 cm^2 cell culture flask. HCT-116 were grown in McCoy's 5a cell media containing 10% FBS and 1% penicillin-streptomycin. Human cancer associated fibroblasts (CAFs) (human primary colorectal tumor CAFs, CAF05) were cultured in a 75 cm^2 cell culture flask. CAFs were grown in either Vitroplus III low serum or MSC-GRO low serum complete cell media. Cell media was changed every 2–3 days. Cells were passaged when a flask reached ~ 90% confluency by first removing the cell media, rinsing with 1x PBS, and incubating at 37° C with 2 mL 0.25% trypsin, 0.53 mM EDTA for 5 min. Then, 8 mL McCoy's or CAF media was added and cells were centrifuged and subcultured at a ratio of 1:3 to 1:8. HCT-116 cells were used for migration assays between passage 7 and passage 17, and CAFs were used for assays between passage 6 and passage 16. All cells were grown at 37° C with 5% CO_2 and 95% humidity. Phenotypic changes of cells were monitored on a brightfield microscope, and cells were counted using a hemocytometer and brightfield microscope.

CAF-conditioned media

CAF-conditioned media was harvested by first growing CAFs following the standard cell culture procedure above. After 72 h, conditioned MSC-GRO media was removed from the culture flask and filtered through a 0.2 μm sterile filter to remove any cell debris. Conditioned media was kept at 4 °C for short-term or − 80 ° C for long-term storage. CAF-conditioned media was used in both the transwell and ibidi μ-slide migration assays. CAF-conditioned media was simply substituted for a traditional chemoattractant molecule dispersed in cell media for each of these assays to characterize HCT-116 response to the full spectrum of CAF signaling molecules. Additionally, CAF-conditioned media was used to culture HCT-116 in certain experiments. HCT-116 was passaged as described above and resuspended and cultured in CAF-conditioned media for 72 h prior to being used for migration assays.

Transwell assay

Transwell migration assays were conducted using the QCM chemotaxis 96-well cell migration assay from Millipore following the manufacturer's protocol. First, 150 μL of the chemoattractant solution in serum-free McCoy's media was added to the lower chamber. For control experiments, serum-free media alone (no chemoattractant) was added to the lower chamber. For experiments with specific chemoattractants, chemoattractant molecules (activin A, TGF-β, CXCL12) were suspended in serum-free McCoy's at various concentrations (activin A: 0-150 ng/mL, TGF-β: 0-100 ng/mL, CXCL12: 0–35 ng/mL) prior to being added to the lower transwell chamber. Conditioned media experiments were conducted by harvesting CAF-conditioned media as described above and diluting it with serum-free McCoy's to the desired concentration prior to adding it to the lower chamber. Finally, crosstalk experiments with CAFs in the lower chamber were conducted by resuspending CAFs in serum-free McCoy's at the desired concentration prior to being added to the assay chamber. After filling the lower assay chamber with the chemoattractant of interest, the upper migration chamber was gently placed on top. This was then filled with 100 μL of $2.5–5.0 \times 10^5$ cells/mL HCT-116 suspended in serum-free McCoy's. The assay plate was then covered and incubated at 37 ° C and 5% CO_2 for 48 h.

Following the 48-h incubation, the cells and media remaining in the top migration chamber were discarded by gently flipping the migration chamber onto a paper towel. The migration chamber was then placed in a fresh 96 well detachment tray containing 150 μL of the prewarmed cell detachment solution and incubated at 37 °C for 30 min. Cells were dislodged from the bottom of the migration chamber by gently tilting the chamber several times during incubation. The migration chamber was removed and 50 μL lysis buffer/CyQuant GR dye solution was added to the 150 μL cell detachment solution. This was allowed to rest for 15 min at room temperature before 150 μL of the mixture was transferred to an opaque black 96-well plate and fluorescence was read on a

plate reader (excitation: 480 nm, emission: 520 nm). For transwell assays in which CAFs were at the bottom and HCT-116 cells were at the top, background fluorescence from the number of CAF cells was subtracted (both sets of cells show similar RFU values for the same cell concentration, and doubling of HCT-116 cell concentration in a co-culture does not change the proliferation of CAFs).

μ-Slide chemotaxis assay

Chemotaxis assays were conducted using the chemotaxis μ-slide from Ibidi following manufacturer protocol. First, cell media and the μ-slide were preincubated at 37 °C and 5% CO_2 overnight. HCT-116 cells were seeded at a density of 3×10^6 cells/mL in a 1.5 mg/mL type I collagen matrix by mixing 20 μL 10x MEM, 20 μL water, 10 μL 7.5% sodium bicarbonate, 50 μL serum-free McCoy's, 150 μL 3 mg/mL collagen, and 50 μL 18×10^6 cells/mL HCT-116. This solution was added to the appropriate channel on the μ-slide and allowed to polymerize at 37 °C and 5% CO_2 for 45 min. Once the collagen matrix was solidified, cells were exposed to solutions of interest by adding 65 μL to the exposure reservoirs on either side of the collagen matrix.

HCT-116 cell migration was characterized for HCT-116 grown using the standard McCoy's 5a cell media as well as for HCT-116 grown in CAF-conditioned media as described above. In both cases, 65 μL of serum-free McCoy's was added to both reservoirs for the negative control. Additionally, for both culturing methods, CAF-induced migration was tested. For this condition, one reservoir was filled with serum-free McCoy's while the other was filled with 3.2×10^5 cells/mL CAFs in serum-free McCoy's. Finally, CAF-conditioned media was tested as a potential chemoattractant for the standard HCT-116 culture. For this, one reservoir was filled with serum-free McCoy's, and the other was filled with CAF-conditioned media.

Following exposure to solutions of interest, cell migration was monitored on a Zeiss Axio Z1 Observer inverted brightfield microscope. Cell migration was tracked by taking timelapse images every 10 min for 24 h while keeping the assay at 37 °C and 5% CO_2. Chemotaxis was evaluated by calculating two common metrics: center of mass (COM) and forward migratory index (FMI) (Eqs. 1, 2). In Eqs. 1, 2 n represents the total number of cells and $x_{i,\,end}$ represents the x-coordinate of a cell's endpoint, where the x-direction is the same direction as the chemical gradient. In Eq. 2, $d_{i,\,accum}$ represents the total distance a cell has traveled. An FMI of 1.0 would indicate that the cells moved in a straight line to their final position at the end of a certain time.

$$COM_x = \frac{1}{n}\sum_{i=1}^{n}(x_{i,end}) \tag{1}$$

$$FMI_x = \frac{1}{n}\sum_{i=1}^{n}\frac{x_{i,\,end}}{d_{i,\,accum}} \tag{2}$$

HCT-116 / CAF 3D co-culture

HCT-116 / CAF 3D co-culture experiments were conducted using a polydimethylsiloxane (PDMS) mold that was made in-house. The mold contains a central reservoir that is 3 mm in diameter that is connected to four peripheral lobes evenly spaced out along the perimeter of the central reservoir that are each 1 mm in diameter (Fig. 6a). For all experiments, a 100–200 μm HCT-116 spheroid was suspended in a 3D matrix in the central reservoir. For CAF-induced migration experiments, one of the peripheral lobes contained CAFs. For negative control experiments, no CAFs were present in the 3D matrix.

HCT-116 spheroids were formed by first culturing cells up to ~90% confluency. Next, cells were resuspended at a concentration of 1×10^4 cells/mL and 100 μL of this solution was added to an ultra-low attachment 96-well plate (InSphero Inc.). The 96 well-plate was then incubated at 37 °C and 5% CO_2 for 3–4 days until a firm spheroid 100–200 μm in diameter formed in each well. Spheroids were then removed via pipetting and used for further experiments.

To fill the PDMS mold with the 3D collagen matrix, a 2 mg/mL collagen type I (rat-tail collagen I, Corning) solution was made by mixing 10 μL 10x MEM cell media, 10 μL sterile water, 5 μL 7.5% sodium bicarbonate, 75 μL 3 mg/mL type I collagen, and 25 μL 5×10^5 cells/mL CAFs or serum-free McCoy's media. For CAF-induced migration experiments, 1 μL of CAF-containing collagen was added to one of the peripheral lobes in the mold; all other lobes were then filled with blank (no CAFs) collagen. For negative control experiments, all peripheral lobes were filled with blank collagen. This was then allowed to polymerize at 37 °C and 5% CO_2 for 15 min. Next, the central reservoir was flooded with blank collagen by adding 3.5 μL, and the HCT-116 spheroid was gently injected into the center of the mold. This was allowed to fully solidify at 37 °C and 5% CO_2 for 45 min. HCT-116 migration was then monitored via brightfield microscopy on an IX81 Olympus microscope equipped with an environment control chamber, and timelapse images were taken every 5 minutes for 48 h.

Mechanical stress experiments

HCT-116 spheroids were formed, and blank (no CAFs) collagen was made as described above. The HCT-116 spheroid was then suspended in the collagen solution and 3 μL of this mixture was carefully pipetted onto the PDMS micro stiffness sensor designed in-house and described previously[39,44]. This was allowed to incubate for 45 min at 37 °C and 5% CO_2 and 95% humidity to prevent collagen drying. After polymerization of collagen, culture media was added. The whole setup was placed on the microscope in a humidity-temperature-controlled chamber. The sample was then stretched, so that collagen fibers were aligned; and the spheroid was monitored using phase-contrast images to track cell migration for 48 h.

Statistical analysis

Transwell HCT-116 migration data was analyzed by first averaging the relative fluorescence readings of a given condition ($n = 3$–6). Average fluorescence readings were then normalized to the serum-free media negative

control (0 ng/mL chemoattractant) to obtain the relative migration enhancement caused by a given condition. μ-slide chemotaxis assays were analyzed using the "Manual Tracking" plugin in ImageJ. For each experimental trial, 20 cells were randomly chosen for tracking. Raw data were processed in the "Chemotaxis and Migration Tool" plugin from ibidi on ImageJ to produce cell trajectory plots and measures of center of mass and forward migratory index. All experimental conditions consisted of three replicates collected on multiple days to ensure reproducibility. For both the transwell and μ-slide chemotaxis assays, Dunnett's multiple comparison test was used to test for statistically significant deviation from the negative (no chemoattractant, no CAFs) control. Statistical analysis and plotting were conducted in GraphPad Prism 6.0c and Python.

Instrumentation

Fluorescence readings for transwell chemotaxis assays were taken on a SpectraMax M2 plate reader (Molecular Devices). Time-lapse brightfield microscopy for μ-slide chemotaxis assays was conducted on a Zeiss Axio Observer Z1 inverted microscope with incubation chamber, CO_2 sensor, and heated stage. Timelapse brightfield images for 3D co-culture and mechanical stress experiments were taken on an Olympus IX81 microscope with incubation chamber, CO_2 sensor, and heated stage. Confocal reflectance images of collagen fibers were obtained with a Zeiss LSM 710 confocal microscope.

Results

HCT-116 migration is not influenced by chemoattractant gradients

In order to assess the potential for chemical control of HCT-116 cell migration, three chemoattractants known to induce migration in colorectal cancer cells[22,28,29] were tested for their impact on HCT-116 cells. HCT-116 migratory response to Activin A, TGF-β, and CXCL12 was measured using the transwell chemotaxis assay, in which the fluorescence readout is proportional to how many cells have traversed the transwell membrane to the chemoattractant-containing chamber (Fig. 1A). HCT-116 cells were plated in the upper migration chamber at a concentration of 5.0×10^4 cells/well, and chemoattractant concentration ranges were chosen based on literature reported values (activin A: 0-150 ng/ml, TGF-β: 0-100 ng/ml, CXCL12: 0–35 ng/ml).[28–30] HCT-116 cell seeding density, assay incubation time, and chemoattractant concentration ranges were refined and optimized in preliminary experiments shown in Figure S1 and Figure S2. Figure 1 shows the chemotactic response of HCT-116 cells exposed to (a) activin a, (b) TGF-β, and (c) CXCL12. All fluorescence measurements were normalized to the 0 ng/mL negative control for each chemoattractant, highlighting the migration enhancement caused by each chemoattractant. For all three chemoattractants tested, there was no statistically significant increase in HCT-116 migration versus the negative control; in fact, some conditions led to less fluorescence signal than the 0 ng/mL control, which is typical in chemotactic systems with very little observed migration. While some increase in cell migration was seen in individual trials of activin A exposure (Fig. S1), these results were unable to be reproduced in further replicates.

Chemotaxis can also be measured at the single-cell level by tracking individual cells upon the introduction of a chemical gradient (Eqs. 1, 2). These experiments were performed in the ibidi μ-slide chemotaxis setup (Fig. 1B) as previously reported by us[45], in the case of activin A and HCT-116. It was suspected that the inconsistent migration enhancement seen in the transwell assay could be caused by activin A increasing overall cell motility rather than chemotaxis per se. Thus, HCT-116 cells were suspended in the 3D collagen matrix in the center of the ibidi μ-slide with 75 ng/mL activin A in one reservoir and serum-free McCoy's media in the other. An activin A concentration of 75 ng/mL was chosen based on the previous results seen in the transwell assay (Fig. 1C). We found that 75 ng/mL activin A caused no change in the center of mass or forward migratory index of HCT-116 cells when compared to the 0 ng/mL negative control (Figure S3). Moreover, there was no change in overall cell speed, debunking the increased motility hypothesis (Figure S3).

Therefore, HCT-116 cells experienced no chemotactic effect caused by the presence of three previously reported chemoattractants: activin A, TGF-β, and CXCL12. This result supports the notion that HCT-116 cell migration—and colorectal cancer cell metastasis—is more complicated than a simple direct migratory response to individual signaling proteins.

Crosstalk is necessary for HCT-116 migration

It has been reported that chemotaxis in certain cell lines relies on cooperativity between multiple signaling molecules to induce directed migration[31–33]. Based on the lack of significant migration in response to single chemoattractants, we suspected HCT-116 migration could follow similar behavior. CAF-conditioned media was harvested from a CAF cell culture after 72 h of incubation and was sterile filtered prior to use in chemotaxis assays. Conditioned media was diluted for use in transwell assays with serum-free McCoy's media. Figure 2 shows HCT-116 migration in response to 5–100% CAF-conditioned media normalized to the 0% conditioned media (100% serum-free McCoy's) negative control. There was no significant enhancement of HCT-116 migration upon exposure to CAF-conditioned media (Fig. 2). Thus, the complex mixture of molecules extracted from CAFs, taken together, does not promote chemotaxis in HCT-116 cells.

We then performed an unusual experiment: we put live CAF cells in the "chemotactic agent" part of the transwell assay, to examine the effect of CAF cell density on HCT-116 migration. In principle, the results of these experiments would not be that different from those of Fig. 2, if the only mechanism of signaling was one-way from molecules produced by CAFs. CAFs were seeded at densities from 6 to 192×10^3 cells/well in serum-free McCoy's media, and HCT-116 migration was measured after 48 h of incubation. The CAF background (no HCT-116) was subtracted from each given condition (Figure S4), and fluorescence readings were normalized to the negative control. Figure 3 shows HCT-116 cell migration in the transwell assay in response to various CAF seeding densities. Significant migration enhancement was seen for CAF concentrations of 12, 24, 48, 96,

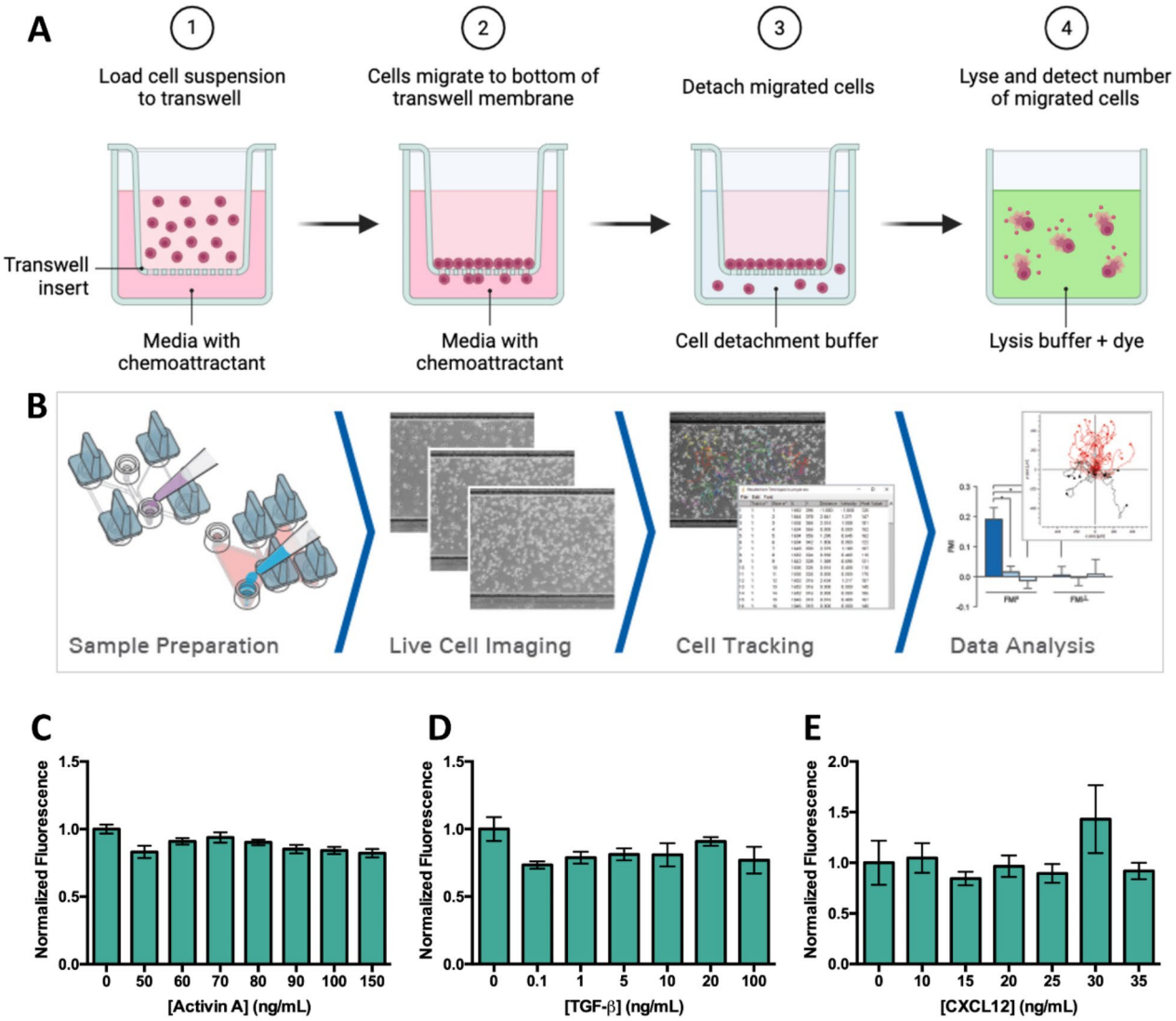

Fig. 1. In vitro migration assays show no clear evidence of chemotactic influence of individual chemoattractants. Schematic of the (**A**) transwell migration assay (created with BioRender.com) and (**B**) ibidi assay where the cancer cells are embedded in 3D collagen with a chemotactic gradient (courtesy of ibidi GmbH). Chemotactic response of HCT-116 cells upon exposure to varying concentrations of three reported chemoattractants: (**C**) Activin A, (**D**) TGF-β, and (**E**) CXCL12. HCT-116 cell migration in the transwell chemotaxis assay (5.0×10^4 cells/well) is quantified by measuring the fluorescence of CyQuant GR dye signal from migrated cells at 520 nm after 48 h. Fluorescence measurements for a given condition are averaged and normalized to the 0 ng/mL negative control ($n = 3$–6). Error bars represent standard error of the mean.

and 192×10^3 CAFs/well (Fig. 3), showing that CAFs plated in the transwell assay reproducibly cause significant HCT-116 migration enhancement.

These results from Figs. 2 and 3 suggest that the signaling network between HCT-116 cells and CAFs might be more complicated than a simple one-way signaling pathway. Instead, it is suspected that CAF-induced migration of HCT-116 may rely on two-way communication between cells, in which the CAF signals cause some sort of response in the HCT-116 cells, which then causes another response in the CAFs. Previous reports have suggested that the CAF-cancer cell crosstalk that occurs in the ECM requires reciprocal communication between the two cell types; this crosstalk has been shown to dynamically change throughout tumor progression which can alter cancer cell behavior[7,9,10,16]. We suspect a reciprocal crosstalk is necessary for the current system; rather than a simple "monologue" of chemical signaling coming from CAFs, a "dialogue" between CAFs and HCT-116 is needed for cell migration enhancement.

CAF-induced migration at the single cell level

The potential for measuring cell-cell crosstalk between HCT-116 and CAFs leading to HCT-116 migration was explored further at the single cell level using the ibidi μ-slide chemotaxis assay. The ibidi μ-slide allows exploration of the interaction between HCT-116 and CAFs in a different system; rather than being entirely

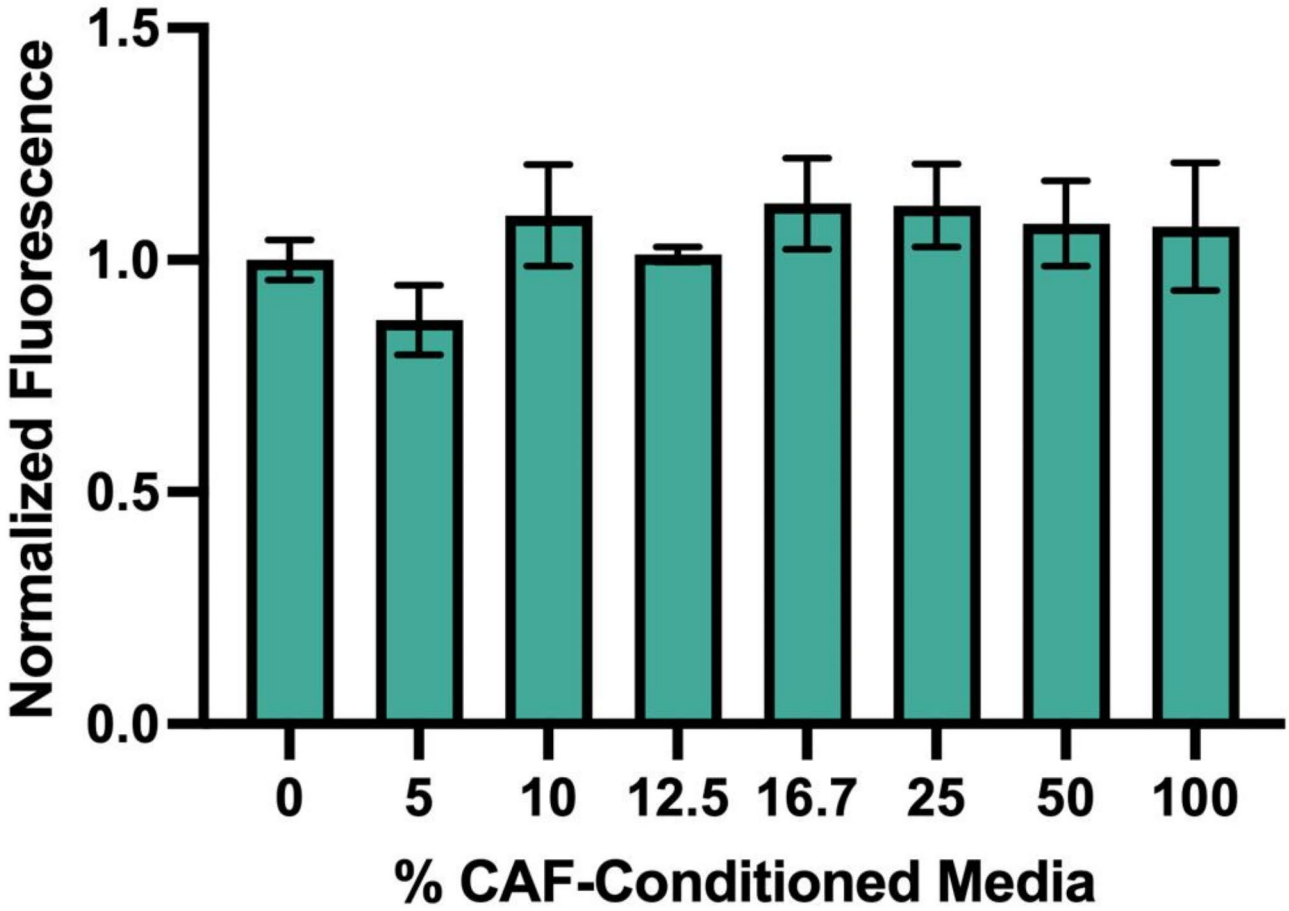

Fig. 2. Chemotactic response of HCT-116 cells upon exposure to 0–100% CAF-conditioned media in serum-free McCoy's media. HCT-116 cell migration in the transwell chemotaxis assay (5.0×10^4 cells/well) is quantified by measuring the fluorescence of CyQuant GR dye signal from migrated cells at 520 nm after 48 h. Fluorescence measurements for a given condition are averaged and normalized to the 0% CAF-conditioned media negative control ($n = 3$–6). Error bars represent standard error of the mean.

solution-based like the transwell assay, the ibidi assay requires HCT-116 cells to be suspended in a 3D collagen matrix prior to being exposed to conditioned media or CAFs in solution (Fig. 1B). Initially, we measured HCT-116 response to CAF-conditioned media compared to serum-free McCoy's media (Table 1). We found that there was no directed migration in response to the CAF-conditioned media, and both the center of mass and forward migratory index for this condition were near zero (Fig. 4a, b). This indicates that in the ibidi assay, CAF-conditioned media does not act as a chemoattractant for HCT-116. Next, we analyzed the ability of CAFs themselves to cause directed migration in the ibidi assay. In the transwell assay, we saw the largest HCT-116 migration enhancement in response to 48×10^3 cells/well (3.2×10^5 cells/mL), which was the CAF concentration used for ibidi assays. Unexpectedly, we saw no directed migration of HCT-116 cells in response to CAFs. Both the center of mass and forward migratory index were near zero for the CAF condition (Fig. 4a, b). This result highlights how the same exposure condition in the transwell and ibidi assays can result in drastically different outcomes. Possible reasons, we hypothesize, could be slow diffusivity or lower bioavailable concentration of chemoattractants in the 3D ibidi assays. Another possible explanation is the difference in pore size in collagen and transwell membrane. 2 mg/mL collagen has a pore diameter of ~3 μm[46], which is smaller than the pores (~8 μm) in the transwell membrane. Moreover, migration in collagen relies on proteolytic degradation, which is not required in transwell migration.

To test whether low concentration is affecting the outcome in ibidi assays, we explored the idea of "priming" HCT-116 cells in the ibidi assay with CAF-conditioned media prior to measuring their cell migration, eliminating the requirement of diffusion of chemoattractants through collagen. The co-culture ibidi assay was unable to produce the same migration enhancement seen in the co-culture transwell assay which we suspect is due to the diffusivity differences in the matrices of the two assays, altering the ability for crosstalk to occur. To try to overcome this problem and observe directed HCT-116 migration in the ibidi assay, we cultured HCT-116 in CAF-conditioned media to allow for long term exposure to CAF chemical secretions. HCT-116 cells were cultured in CAF-conditioned media for 72 h prior to being used for the ibidi chemotaxis assay. Conditioned media cultured HCT-116 were exposed to both serum-free McCoy's media and CAFs and compared to the standard HCT-116 cell culture (Table 1). Figure 4 shows the (a) center of mass and (b) forward migratory index

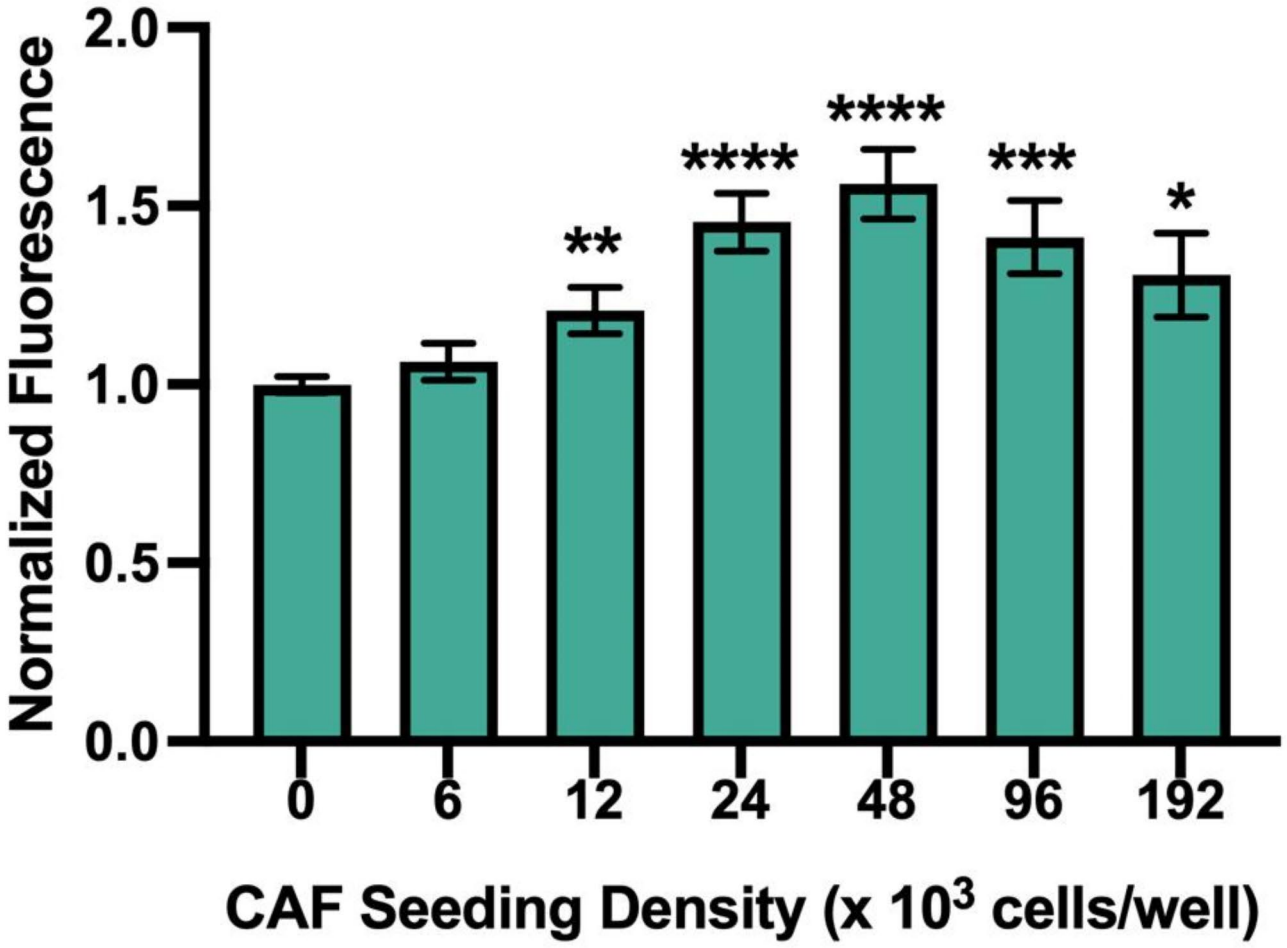

Fig. 3. Chemotactic response of HCT-116 cells upon exposure to living CAFs seeded in serum-free McCoy's media in the bottom of the transwell assay at various densities. HCT-116 cell migration in the transwell chemotaxis assay (5.0×10^4 cells/well) is quantified by measuring the fluorescence of CyQuant GR dye signal from migrated cells at 520 nm after 48 h. Fluorescence measurements for a given condition are background subtracted, averaged, and normalized to the 0% CAF-conditioned media negative control ($n = 8–10$). Error bars represent standard error of the mean.

Experimental condition	Cell culture medium	"Chemoattractant"
HCT-116 / SF*	McCoy's 5a media	Serum-free McCoy's
HCT-116 / CM**	McCoy's 5a media	CAF-cond. media
HCT-116 / CAFs	McCoy's 5a media	320k cells/mL CAFs
CM HCT-116 / SF	CAF-cond. media	Serum-free McCoy's
CM HCT-116 / CAFs	CAF-cond. media	320k cells/mL CAFs

Table 1. Cell culture and chemotaxis assay conditions for single-cell migration experiments. * SF - Serum Free; ** CM - conditioned media from CAFs

of conditioned media HCT-116 experiments. While some conditions produce apparent negative cell migration, both measures of chemotaxis are near zero and are not significantly different from the standard culture / serum-free McCoy's condition, indicating no chemotactic effect from CAFs or CAF-conditioned media. Therefore, priming HCT-116 cells with CAF-conditioned media does not appear to be an effective method for simulating the chemical crosstalk that occurs between these cells.

CAF-induced migration in an HCT-116 tumor spheroid

While the 2D chemotaxis assays conducted above provide valuable insight into the chemical signaling network of HCT-116 and CAFs, they do not provide a complete view of colorectal cancer cell migration. Hence, we conducted CAF-induced HCT-116 migration experiments in a 3D collagen matrix containing a co-culture of an

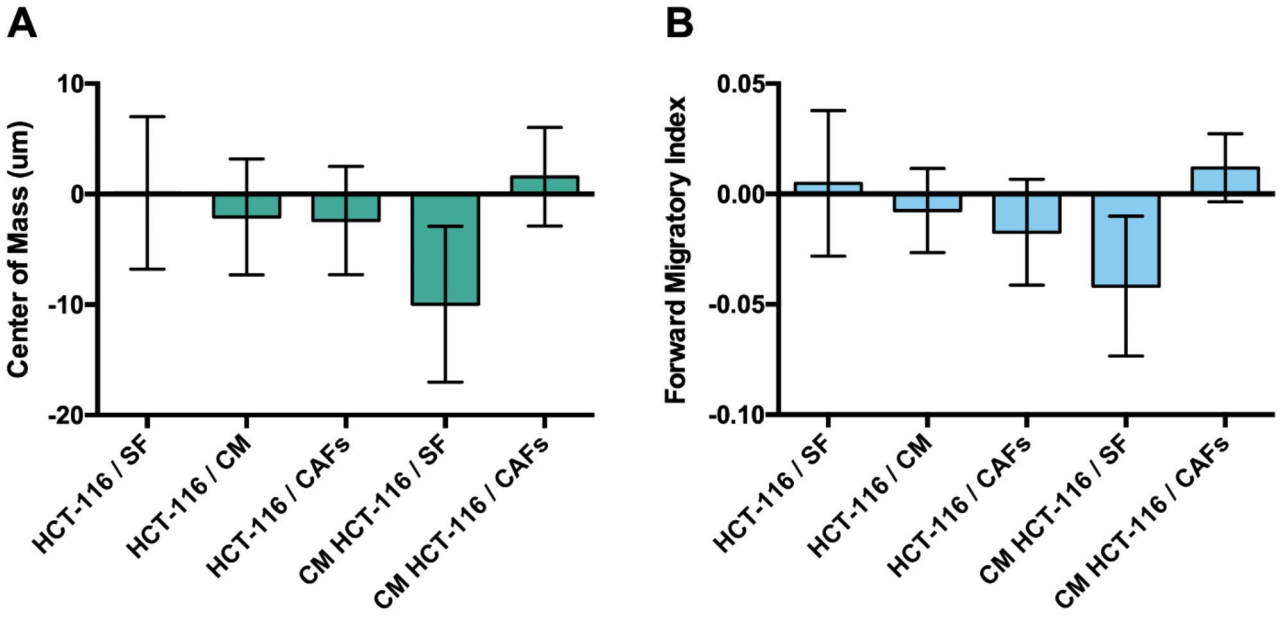

Fig. 4. (**A**) Center of mass (x) and (**B**) forward migratory index (x) for HCT-116 cells cultured using standard and CAF-conditioned cell media. Response to serum-free McCoy's media and 3.2×10^5 cells/mL CAFs in serum-free McCoy's was characterized for standard and conditioned media cultured HCT-116 and response to CAF-conditioned media was characterized for standard cultured HCT-116. Bar heights represent mean values ($n = 3$). Error bars represent standard error of the mean.

HCT-116 tumor spheroid (Fig. 5) and CAFs. By using a fully 3-dimensional matrix, migration assays simulate a more biologically relevant environment that contains both chemical and mechanical microenvironment. Additionally, higher cell densities in HCT-116 spheroids better represent the tumor environment in vivo. As an additional control experiment, CAFs were suspended in a 2 mg/mL collagen matrix at a concentration of 5×10^5 cells/mL and the solution was injected into one of the peripheral lobes of the PDMS collagen mold (Fig. 6a). Following polymerization, the remainder of the mold was filled with 2 mg/mL collagen, and a 100–200 μm HCT-116 spheroid was injected into the center. The gel was allowed to solidify, and HCT-116 cell migration was monitored via brightfield microscopy for 48 h. Figure 6a shows HCT-116 spheroid migration after 2- and 42-hour incubation with CAFs in the 3D co-culture experiment. At 2 h, there are no individual cells visible outside of the HCT-116 spheroid. At 42 h, many individual HCT-116 cells can be seen migrating out of the spheroid toward the upper right corner of the image (where CAFs are located), and the overall size of the spheroid has increased. Figure 6b shows the radial plot of the HCT-116 cell location at different times. The expanding outline of the spheroid demonstrates the overall growth of the spheroid in all directions. However, it is also evident that individual cancer cells were migrating further toward the direction of CAFs, as illustrated by the top-right quadrant of the radial plot (Fig. 6b). Distance migrated by the cancer cells towards the CAFs is ~100% of the initial radius, whereas in other directions, migration distance is significantly shorter (~30% of the initial radius) (Fig. 6b, c). This is remarkably different compared to the random migration observed in the control case without CAFs (Fig. 5).

We imaged the collagen matrix with confocal microscopy and found that CAFs indeed aligned the collagen fibers and cancer cell migration followed the direction of alignment (Fig. 6d). In comparison, collagen fibers are dispersed at random orientations in a matrix without CAFs (Fig. 6d). To ascertain that the alignment is induced by the CAFs, not the cancer cells, we created samples without the cancer spheroids and observed similar fiber alignment. This demonstrates that CAFs induce directional migration in HCT-116 cells, supporting the hypothesis that CAF-cancer cell crosstalk plays an important role in the metastatic progression of colorectal tumors.

Mechanical modulation of HCT-116 Migration

Since the 3D CAF-induced migration observed above could be the product of chemical, mechanical, or a combination of signaling modalities, we wanted to examine how HCT-116 cells respond to a strictly mechanical stimulus. To do so, we suspended HCT-116 spheroids in a 2 mg/mL collagen matrix in the center of an in-house micro stiffness sensor[39,44] and pulled on one end of the sensor with constant force to induce mechanical stress (Fig. 7a). Figure 7b shows the migration of HCT-116 cells in a tumor spheroid after 2- and 36-hour incubation. Figure 7c shows the radial migration plot of HCT-116 cells at different times. After 2 h of mechanical stress, the HCT-116 spheroid still appears fairly spherical, and no individual cells are observed outside of the spheroid (Fig. 7b). However, after 30 h, the spheroid has elongated along the axis of mechanical stress, and some individual cells can be seen leaving the spheroid (Fig. 7b, c). Figure 7d shows that cell migration in regions under tensile stress is significantly higher compared to other regions in collagen. This experiment demonstrates that HCT-116

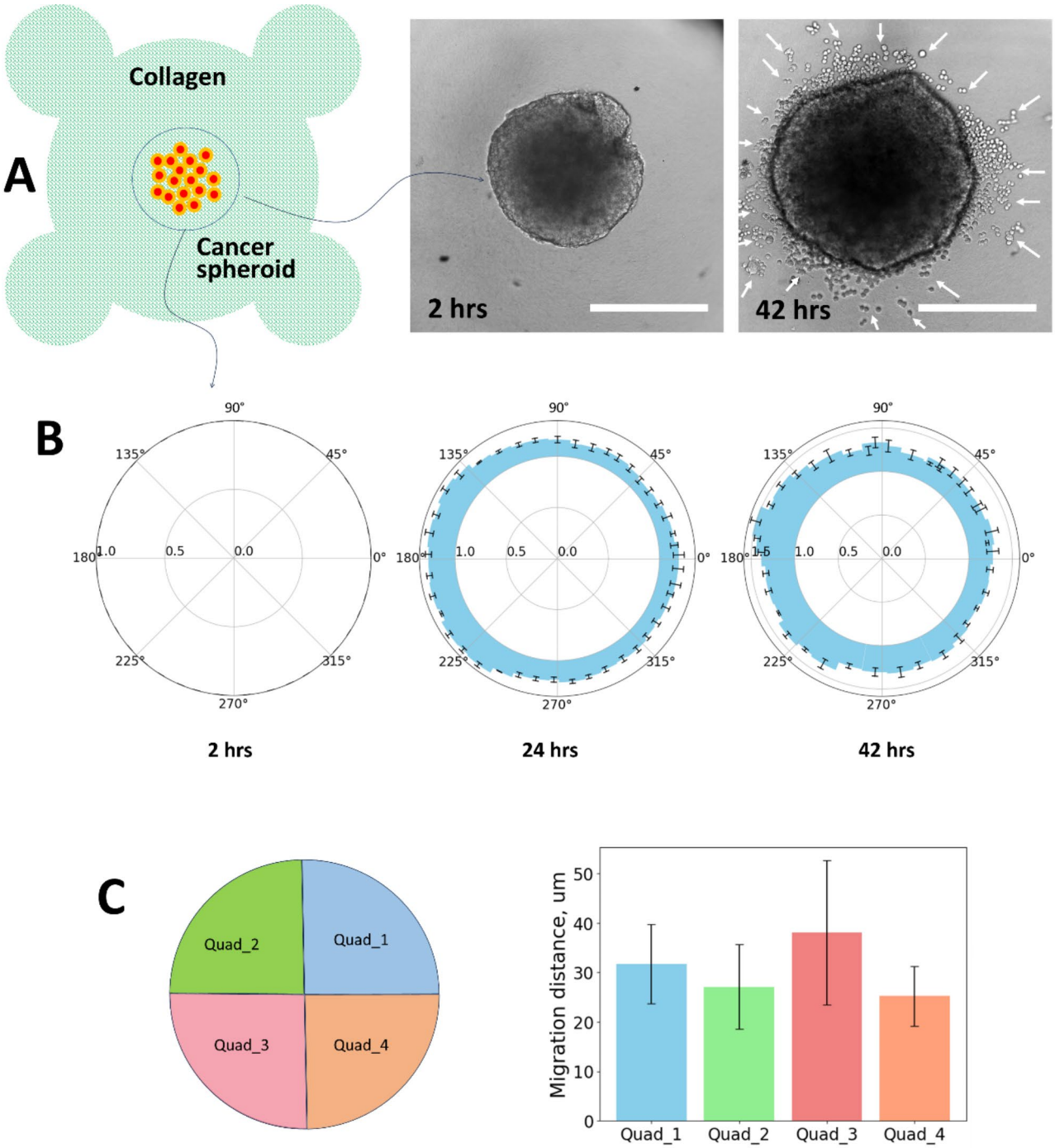

Fig. 5. Cancer cells migrate from the spheroids randomly in all directions. (**a**) The HCT-116 spheroids were placed at the center. Brightfield images after 2 and 42 h of incubation show the HCT-116 spheroids and individual cells that migrated out (white arrows). Scale bars: 100 µm. (**b**) Longitudinal radial plot of HCT-116 cell migration. Concentric circles on the x-axis represent migration distance (normalized to the initial radius). (**c**) Comparison of migration distance between different quadrants. Migration of cancer cells in all quadrants is statistically similar, indicating that cancer cells do not migrate toward any preferred direction. Bar heights in radial plots represent mean values ($n = 3$). Error bars represent the standard error of the mean.

cell migration can be controlled by purely mechanical cues. Directed migration by HCT-116 cells in response to a mechanically induced fiber alignment, in the absence of chemical signaling from CAFs, provides clear evidence that matrix mechanics play a crucial role in colorectal cancer cell migration.

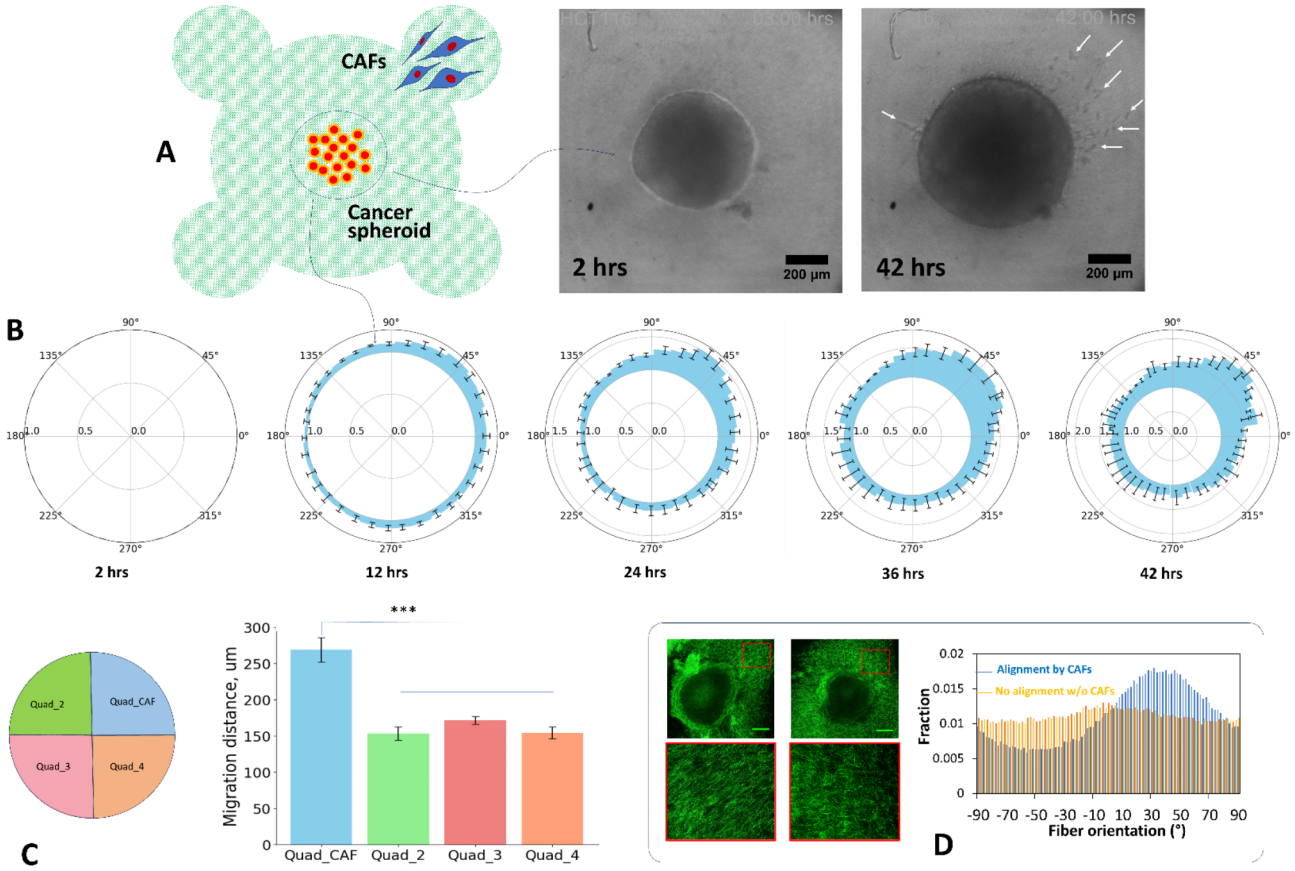

Fig. 6. CAFs induce directional migration of cancer cells. (**a**) Experimental setup for investigating how CAFs influence HCT-116 cancer cell migration. The HCT-116 spheroids were placed at the center, with the CAFs located at the top-right. Brightfield images after 2 and 42 h of incubation show the HCT-116 spheroids and individual cells that migrated out (white arrows). Scale bars: 200 µm. (**b**) Longitudinal radial plot of HCT-116 cell migration. Concentric circles on the x-axis represent migration distance (normalized to the initial radius). It is evident that CAFs (at 45°) induced increased cancer cell migration towards their location. (**c**) Comparison of migration distance between different quadrants. Migration of cancer cells in the quadrant containing CAFs is significantly higher than in the control quadrants without CAFs. (**d**) Confocal reflectance microscopy images and fiber alignment histograms reveal that CAFs significantly aligned the collagen fibers at ~45°. In contrast, samples without CAFs demonstrate a uniform distribution of fiber alignment. Scale bars: 100 µm. Bar heights in radial plots represent mean values ($n = 4$). Error bars represent the standard error of the mean.

Discussion

Here, we attempted to deconvolute the chemical from mechanical control of HCT-116 migration and colorectal cancer cell metastasis. Colorectal cancer metastasis has been shown previously to be influenced by both chemical and mechanical signals produced by CAFs in the ECM. We extensively characterized the chemotactic response of HCT-116 to CXCL12, TGF-β, and activin A—three reported colorectal cancer cell chemoattractants—in two analytical chemotaxis assays. While some individual replicates yielded chemotaxis results in accordance with previous literature, further experiments produced results deviating from previous reports of these factors enhancing colorectal cancer cell migration. For example, CXCL12 is frequently associated with increased migration and poor patient outcomes in colorectal cancer[47], but failed to induce chemotaxis in our assays. Similarly, TGF-β and activin A, well-documented drivers of epithelial-mesenchymal transition and migration in other systems[22,48], did not elicit significant chemotactic behavior in our study. This divergence highlights the potential complexity and context-dependence of chemokine signaling. It may also reflect the importance of additional cofactors, matrix interactions, or heterotypic signaling as noted in prior studies[20,47].

We also tested for chemotaxis in HCT-116 cells in response to CAF chemical secretions representing one-way signaling (CAF-conditioned media) and two-way signaling (CAFs co-culture in chemotaxis assays). Interestingly, we found that while HCT-116 cells experienced very little to no enhancement of cell migration when exposed to CAF-conditioned media, HCT-116 cells exposed to CAFs that were seeded in the chemoattractant chamber of the transwell assay experienced strong migration enhancement, suggesting a two-way "dialogue" between CAFs and HCT-116 cells may be required for chemically-induced migration. However, in an alternate chemotaxis assay (ibidi µ-slide assay), CAF-conditioned media and CAF co-cultured in the assay had no impact on HCT-116 migration, possibly due to weak chemical gradient and different migration mechanics. By testing for HCT-

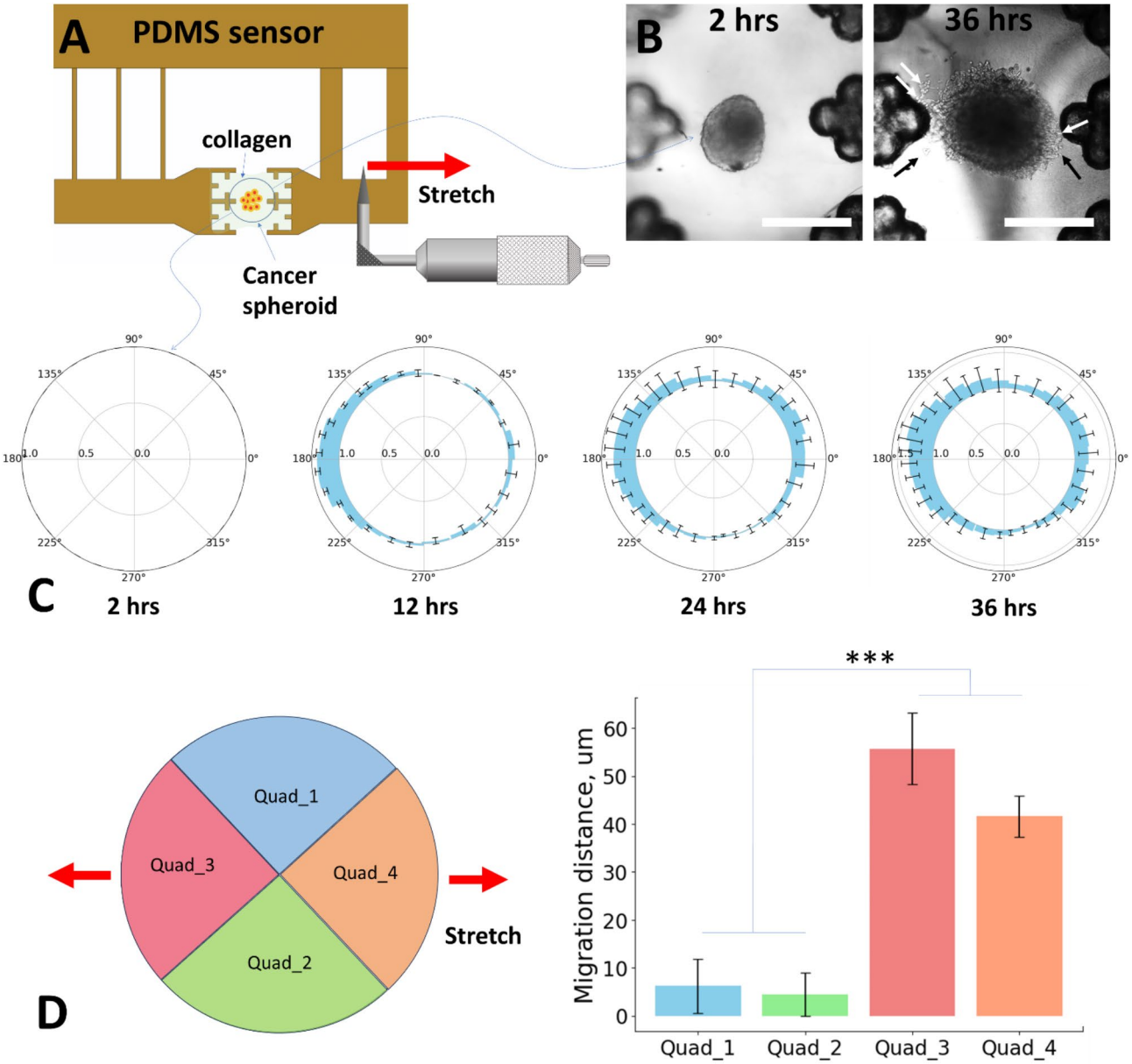

Fig. 7. Mechanical alignment of collagen fibers induces directional migration of cancer cells. (**A**) Experimental setup for stretching a specimen of collagen matrix with a cancer spheroid. The HCT-116 spheroids were placed at the center of the sample. (**B**) Brightfield images after 2 and 36 h of incubation show the HCT-116 spheroids and individual cells that migrated out (indicated by arrows). Scale bars: 500 µm. (**C**) Longitudinal radial plot of HCT-116 cell migration. Concentric circles on the x-axis represent migration distance (normalized to initial radius). It is evident that cells were migrating at a higher rate in the direction of stretch and fiber alignment (0° and 180°). (**D**) Comparison of migration distance between different quadrants. Migration of cancer cells in the quadrants in tension is significantly higher than in the other two quadrants. Bar heights in radial plots represent mean values ($n = 4$). Error bars represent standard error of the mean.

116 migratory response to chemoattractants, CAF-conditioned media, and CAFs themselves, we demonstrated that chemically-induced HCT-116 migration may be more complex and dynamic than previously thought.

Additionally, we conducted experiments to characterize HCT-116 tumor spheroid migration in response to CAFs in a fully 3-dimensional, more biologically, relevant assay. We found that HCT-116 cells directionally migrated to the ECM region containing CAFs, demonstrating the directional influence CAFs have on HCT-116 migration. Finally, we analyzed the migratory response of HCT-116 to an artificial mechanical strain; we found that by introducing mechanical stress and collagen fiber alignment to the ECM, HCT-116 cells migrate along the axis of mechanical strain. We suspect that the migratory response of HCT-116 cells to CAFs is largely due to mechanical forces rather than chemical signaling, but this complex, dynamic cellular crosstalk must be further examined.

Our results support a growing body of evidence that mechanical factors play a dominant role in colorectal cancer metastasis. CAFs are known to stiffen the ECM through collagen crosslinking and alignment, promoting contact guidance and durotaxis[49–53]. In agreement, we observed significant directional migration of HCT-116 cells along mechanically strained collagen fibers. This finding is consistent with broader observations that aligned collagen fibers serve as migration tracks, facilitating cancer invasion[54,55]. Furthermore, the stiffened ECM resulting from CAF activity is closely linked to increased metastatic potential in colorectal and other cancers. Our artificial mechanical strain experiments demonstrated that HCT-116 cells migrate preferentially along strain axes, highlighting the importance of contact guidance in mediating tumor cell behavior. These results suggest that mechanical properties of the tumor microenvironment, shaped by fibroblast activity, may outweigh direct chemical signaling in influencing cancer cell migration.

Our findings suggest that the interplay between CAFs and cancer cells is more complex than simple chemical or mechanical signaling alone. CAF-mediated ECM remodeling appears to provide the structural cues necessary for directional migration, while chemical signaling requires dynamic crosstalk to achieve significant migratory enhancement. These insights into the mechanical and chemical influences on colorectal cancer metastasis may have implications for therapeutic strategies. Targeting ECM stiffness and CAF-mediated remodeling could complement traditional approaches aimed at inhibiting chemokine signaling pathways. Additionally, incorporating mechanobiological parameters into drug screening platforms may yield more effective therapies by capturing the dynamic nature of tumor cell migration.

Data availability

The datasets generated and/or used in this study will be available from the Illinois Data Bank (databank.illinois.edu).

Received: 13 October 2024; Accepted: 3 February 2025
Published online: 10 February 2025

References

1. Hossain, M. S. et al. Colorectal cancer: A review of carcinogenesis, global epidemiology, current challenges, risk factors, preventive and treatment strategies. *Cancers (Basel)*. **14**, 1–25 (2022).
2. Papamichael, D. et al. Treatment of colorectal cancer in older patients: International Society of Geriatric Oncology (SIOG) consensus recommendations 2013. *Ann. Oncol.* **26**, 463–476 (2015).
3. Siegel, R. L. et al. Colorectal Cancer incidence patterns in the United States, 1974–2013. *J. Natl. Cancer Inst.* **109**, 1–6 (2017).
4. Siegel, R. L., Miller, K. D. & Jemal, A. Cancer statistics, 2018. *CA Cancer J. Clin.* **68**, 1–30 (2018).
5. Yin, Y. & Tian, X. Colorectal cancer mortality rates in adults aged 20 to 54 years in the United States, 1970–2014. *J. Am. Med. Assoc.* **318**, 572–574 (2017).
6. Sleeboom, J. J. F. et al. The extracellular matrix as hallmark of cancer and metastasis: From biomechanics to therapeutic targets. *Sci. Transl Med.* **16**, 1–16 (2024).
7. Salemme, V., Centonze, G., Cavallo, F., Defilippi, P. & Conti, L. The crosstalk between tumor cells and the immune microenvironment in breast cancer: Implications for immunotherapy. *Front. Oncol.* **11**, 1–20 (2021).
8. Alves, A. et al. Tumor microenvironment and oral squamous cell carcinoma: A crosstalk between the inflammatory state and tumor cell migration. *Oral Oncol.* **112**, 1–8 (2021).
9. Jahanafrooz, Z. et al. Colon cancer therapy by focusing on colon cancer stem cells and their tumor microenvironment. *J. Cell. Physiol.* **235**, 4153–4166 (2020).
10. Fares, J., Fares, M. Y., Khachfe, H. H., Salhab, H. A. & Fares, Y. Molecular principles of metastasis: A hallmark of cancer revisited. *Signal. Transduct. Target. Therapy*. **5**, 1–17 (2020).
11. Bissell, M. J. & Hines, W. C. Why don't we get more cancer? A proposed role of the microenvironment in restraining cancer progression. *Nat. Med.* **17**, 320–329 (2011).
12. Hanahan, D. & Coussens, L. M. Accessories to the crime: Functions of cells recruited to the tumor microenvironment. *Cancer Cell.* **21**, 309–322 (2012).
13. Muller, A. et al. Involvement of chemokine receptors in breast cancer metastasis. *Nature* **410**, 50–56 (2001).
14. Petrova, V., Annicchiarico-Petruzzelli, M., Melino, G. & Amelio, I. The hypoxic tumour microenvironment. *Oncogenesis* **7**, 1–13 (2018).
15. Carloni, V., Luong, T. V. & Rombouts, K. Hepatic stellate cells and extracellular matrix in hepatocellular carcinoma: More complicated than ever. *Liver Int.* 834–843 (2014).
16. Kalluri, R. The biology and function of fibroblasts in cancer. *Nat. Rev. Cancer* vol. 16 582–598 Preprint at (2016). https://doi.org/10.1038/nrc.2016.73
17. Räsänen, K. & Vaheri, A. Activation of fibroblasts in cancer stroma. *Exp. Cell. Res.* **316**, 2713–2722 (2010).
18. Yamaguchi, H. & Sakai, R. Direct interaction between carcinoma cells and cancer associated fibroblasts for the regulation of cancer invasion. *Cancers (Basel)*. **7**, 2054–2062 (2015).
19. Karagiannis, G. S. et al. Cancer-associated fibroblasts drive the progression of metastasis through both paracrine and mechanical pressure on cancer tissue. *Mol. Cancer Res.* **10**, 1403–1418 (2012).
20. Emon, B., Bauer, J., Jain, Y., Jung, B. & Saif, T. Biophysics of tumor microenvironment and cancer metastasis: A mini review. *Comput. Struct. Biotechnol. J.* **16**, 279–287 (2018).
21. Schmitt, M. & Greten, F. R. The inflammatory pathogenesis of colorectal cancer. *Nat. Rev. Immunol.* **21**, 653–667 (2021).
22. Bauer, J. et al. Increased stiffness of the tumor microenvironment in colon cancer stimulates cancer associated fibroblast-mediated prometastatic activin A signaling. *Sci. Rep.* **10**, 1–11 (2020).
23. Malki, A. et al. Molecular mechanisms of colon cancer progression and metastasis: recent insights and advancements. *Int. J. Mol. Sci.* **22**, 1–24 (2021).
24. Jia, S. N., Han, Y. B., Yang, R. & Yang, Z. C. Chemokines in colon cancer progression. *Semin Cancer Biol.* **86**, 400–407 (2022).
25. Pączek, S., Łukaszewicz-Zając, M. & Mroczko, B. Chemokines—What is their role in colorectal cancer? *Cancer Control.* **27**, 1–8 (2020).
26. Bhattacharya, R. et al. Intracrine VEGF signalling mediates colorectal cancer cell migration and invasion. *Br. J. Cancer*. **117**, 848–855 (2017).
27. Principe, D. R. et al. Loss of TGFβ signaling promotes colon cancer progression and tumor-associated inflammation. *Oncotarget* **8**, 3826–3839 (2017).

28. Han, S. et al. Dexamethasone inhibits TGF-β1-induced cell migration by regulating the ERK and AKT pathways in human colon cancer cells via CYR61. *Cancer Res. Treat.* **48**, 1141–1153 (2016).
29. Akishima-Fukasawa, Y. et al. Prognostic significance of CXCL12 expression in patients with colorectal carcinoma. *Am. J. Clin. Pathol.* **132**, 202–210 (2009).
30. Bauer, J. et al. Activin and TGFβ use diverging mitogenic signaling in advanced colon cancer. *Mol. Cancer*. **14**, 1–14 (2015).
31. Loomans, H. A. & Andl, C. D. Intertwining of activin a and TGFβ signaling: dual roles in cancer progression and cancer cell invasion. *Cancers (Basel)*. **7**, 70–91 (2015).
32. Staudacher, J. J. et al. Activin signaling is an essential component of the TGF-β induced pro-metastatic phenotype in colorectal cancer. *Sci. Rep.* **7**, 1–9 (2017).
33. Zessner-Spitzenberg, J., Thomas, A. L., Krett, N. L. & Jung, B. TGFβ and activin A in the tumor microenvironment in colorectal cancer. *Gene Rep.* **17**, 1–20 (2019).
34. Mohammadi, H. & Sahai, E. Mechanisms and impact of altered tumour mechanics. *Nat. Cell Biol.* **20**, 766–774 (2018).
35. Kalli, M. & Stylianopoulos, T. Defining the role of solid stress and matrix stiffness in cancer cell proliferation and metastasis. *Front. Oncol.* **8**, 1–7 (2018).
36. Rice, A. J. et al. Matrix stiffness induces epithelial-mesenchymal transition and promotes chemoresistance in pancreatic cancer cells. *Oncogenesis* **6**, 1–9 (2017).
37. Tang, X. et al. A mechanically-induced colon cancer cell population shows increased metastatic potential. *Mol. Cancer*. **13**, 1–15 (2014).
38. Kawano, S. et al. Assessment of elasticity of colorectal cancer tissue, clinical utility, pathological and phenotypical relevance. *Cancer Sci.* **106**, 1232–1239 (2015).
39. Emon, B. et al. A novel method for sensor-based quantification of single/multicellular force dynamics and stiffening in 3D matrices. *Sci. Adv.* **7**, 1–11 (2021).
40. Ali, M. Y., Chuang, C. Y. & Saif, M. T. A. Reprogramming cellular phenotype by soft collagen gels. *Soft Matter*. **10**, 8829–8837 (2014).
41. Tang, X. et al. Mechanical force affects expression of an in vitro metastasis-like phenotype in HCT-8 cells. *Biophys. J.* **99**, 2460–2469 (2010).
42. Grzincic, E. M. & Murphy, C. J. Gold Nanorods indirectly promote Migration of Metastatic human breast Cancer cells in three-dimensional cultures. *ACS Nano*. **9**, 6801–6816 (2015).
43. Castro-Abril, H. et al. The role of Mechanical properties and structure of type I collagen hydrogels on colorectal cancer cell migration. *Macromol. Biosci.* **23**, 1–18 (2023).
44. Emon, B., Joy, M. S. H. & Saif, M. T. A. Developing a multi-functional sensor for cell traction force, matrix remodeling and biomechanical assays in self-assembled 3D tissues in vitro. *Protoc. Exch.* 1–34 (2021).
45. Tetrick, M. G. & Murphy, C. J. Leveraging tunable nanoparticle surface functionalization to alter cellular migration. *ACS Nanosci. Au*. **4**, 205–215 (2024).
46. Hall, M. S. et al. Fibrous nonlinear elasticity enables positive mechanical feedback between cells and ECMs. *PNAS* 113, (2016).
47. Goïta, A. A. & Guenot, D. Colorectal cancer: The contribution of CXCL12 and its receptors CXCR4 and CXCR7. *Cancers (Basel)*. **14**, 1810 (2022).
48. Staudacher, J. J. et al. Activin signaling is an essential component of the TGF-β induced pro-metastatic phenotype in colorectal cancer. *Sci. Rep.* **7**, (2017).
49. Levental, I. et al. A simple indentation device for measuring micrometer-scale tissue stiffness. *J. Phys. Condens. Matter*. **22**, 194120 (2010).
50. Levental, K. R. et al. Matrix crosslinking forces tumor progression by enhancing integrin signaling. *Cell* **139**, 891–906 (2009).
51. Provenzano, P. P., Inman, D. R., Eliceiri, K. W., Trier, S. M. & Keely, P. J. Contact guidance mediated three-dimensional cell migration is regulated by Rho/ROCK-dependent matrix reorganization. *Biophys. J.* **95**, 5374 (2008).
52. Ray, A., Slama, Z. M., Morford, R. K., Madden, S. A. & Provenzano, P. P. Enhanced directional migration of cancer stem cells in 3D aligned collagen matrices. *Biophys. J.* **112**, 1023 (2017).
53. Shieh, A. C., Rozansky, H. A., Hinz, B. & Swartz, M. A. Tumor cell invasion is promoted by interstitial flow-induced matrix priming by stromal fibroblasts. *Cancer Res.* **71**, 790–800 (2011).
54. Ray, A. & Provenzano, P. P. Aligned forces: origins and mechanisms of Cancer Dissemination guided by ECM Architecture. *Curr. Opin. Cell. Biol.* **72**, 63 (2021).
55. Riching, K. M. et al. 3D collagen alignment limits protrusions to enhance breast cancer cell persistence. *Biophys. J.* **107**, 2546–2558 (2014).

Acknowledgements

We thank the Cancer Center at Illinois Seed Grant no. 9570 for financial support. This material is based upon work supported by the National Science Foundation (NSF) Graduate Research Fellowship under Grant No. DGE 21-46756. This study was also partially funded by NSF grant ECCS 1934991 and the Chan Zuckerberg Biohub Chicago. We thank Dr. Sandy McMasters from the UIUC cell media facility for her help in preparing cell culture materials. Confocal images were taken at the core facilities of Institute for Genomic Biology at UIUC.

Author contributions

C. J. M. and M. T. A. S. conceived the ideas and designed experiments. M. G. T., M. A. B. E., U. D., M. M., J. S. and V. R. performed experiments, analyzed data, and created figures and tables. All authors contributed to the writing of the manuscript.

Declarations

Competing interests

The authors declare no competing interests.

Additional information

Supplementary Information The online version contains supplementary material available at https://doi.org/10.1038/s41598-025-89152-4.

Correspondence and requests for materials should be addressed to C.J.M.

Reprints and permissions information is available at www.nature.com/reprints.